ORIGINAL RESEARCH

Pattern and Prognostic Implications of Cardiac Metastases Among Patients With Advanced Systemic Cancer Assessed With Cardiac Magnetic Resonance Imaging

Shawn C. Pun, MD; Andrew Plodkowski, MD; Matthew J. Matasar, MD; Yulia Lakhman, MD; Darragh F. Halpenny, MD; Dipti Gupta, MD; Chaya Moskowitz, PhD; Jiwon Kim, MD; Richard Steingart, MD; Jonathan W. Weinsaft, MD

***Background*—**Cardiac magnetic resonance (CMR) imaging is well validated for tissue characterization of cardiac masses but has not been applied to study pattern and prognostic implications of cardiac metastases (CMETs) among patients with systemic cancer.

***Methods and Results*—**The population consisted of 60 patients with stage IV cancer (32 patients with CMETs, 28 diagnosis-matched controls) undergoing CMR. CMET was defined as a discrete mass with vascular tissue properties on delayed enhancement CMR. CMET-positive patients and controls had similar clinical characteristics, cardiac geometry, and function (P=NS). Leading cancer types associated with CMET were sarcoma, melanoma, and gastrointestinal. Patients with CMETs had similar distribution of extracardiac metastatic disease compared with controls (organs involved: 3.4±2.0 versus 2.7±1.9, P=0.17). In 94% of patients with CMETs, there were metastases involving ≥1 extracardiac organ (66% lung involvement). CMET location varied (right ventricle 44%, right atrium 19%, left ventricle 28%, left atrium 9%, pericardial 25%); 22% of cases had multichamber involvement. Right-sided chamber involvement was common in hematologic/lymphatic spread (67%); pericardial involvement was common with direct spread (64%). Regarding tissue properties on delayed enhancement CMR, CMETs commonly (59%) demonstrated heterogeneous enhancement (41% diffuse enhancement). Heterogeneous lesions were larger and had increased border irregularity (P<0.05). Survival 6 months post-CMR was numerically lower among patients with CMETs (56% [95% CI 39–74%]) versus stage IV cancer–matched controls (68% [95% CI 50–86%]), although differences between groups were nonsignificant (P=0.42).

***Conclusions*—**CMETs vary regarding etiology, location, and tissue properties on CMR, highlighting need for comprehensive surveillance of cardiac involvement regardless of cancer origin. Prognosis remains poor with for patients with CMETs, albeit similar to that for stage IV cancer controls matched for cancer etiology. **(*J Am Heart Assoc*. 2016;5:e003368 doi: 10.1161/JAHA.116.003368)**

Key Words: cardiac metastases • cardiac tumor • cardio-oncology • cardiovascular magnetic resonance • oncology

Among patients with systemic cancer, cardiac metastases (CMETs) are an important complication that can affect clinical decision-making. Current understanding of the prevalence and pattern of CMETs is limited. Most data regarding cancer in the heart are derived from autopsy series[1,2] and may reflect selected patient populations with advanced disease at time of death. In vivo studies have largely used echocardiography,[3] which is known to yield varying test performance based on image quality and be limited for the detection of cardiac masses that are small or nonprotuberant.[4,5] Regardless of diagnostic approach, recent advances in oncologic care may correspond to altered patterns of cancer spread to the heart, as well as improved prognosis. However, pattern and prognostic significance of CMETs among patients receiving contemporary anticancer therapies is not well established.

Cardiac magnetic resonance (CMR) imaging provides high-resolution assessment of cardiac structure and function. Of particular relevance to CMETs, CMR provides reproducible cross-sectional assessment of cardiac geometry,[6] enabling comprehensive assessment of CMET location and functional sequelae. Beyond anatomic imaging, CMR enables tissue characterization of cardiac masses based on vascular supply.

From the Departments of Medicine (S.C.P., M.J.M., D.G., R.S., J.W.W.), Radiology (A.P., Y.L., D.F.H.), and Epidemiology and Biostatistics (C.M.), Memorial Sloan Kettering Cancer Center, New York, NY; Department of Medicine, Weill Cornell Medical College, New York, NY (J.K., J.W.W.).

Correspondence to: Jonathan W. Weinsaft, MD, Medicine in Radiology, Cardiac Magnetic Resonance Imaging Program, Weill Cornell Medicine, Memorial Sloan Kettering Cancer Center, 525 E 68th St, New York, NY 10021. E-mail: jww2001@med.cornell.edu

Received February 9, 2016; accepted March 28, 2016.

Differentiation of neoplasm from thrombus based on contrast uptake has been validated in relation to histopathology findings.[7–9] Tissue characterization imaging of masses has also been shown to stratify clinical outcomes.[4] CMR is increasingly used to assess cancer patients and has been used to study mixed patient cohorts with benign and malignant neoplasms.[10,11] To date, CMR has not been used to study CMETs among patients with systemic cancer.

This study used a tailored CMR protocol—including dedicated tissue characterization imaging—to study anatomic pattern, tissue properties, and prognostic implications of CMETs in the current era. Aims were as follows: (1) identify common cancer types and clinical indices associated with CMETs; (2) assess anatomic location, mode of spread, and contrast-enhanced tissue properties of CMETs; and (3) determine prognosis of patients with CMETs compared with controls matched for primary cancer type.

Methods

Study Population

The population included consecutive adults (≥18 years old) with extracardiac cancer and CMETs as identified through the use of delayed enhancement (DE-)CMR. Established criteria were used to distinguish CMETs from thrombi[4,7,8]: CMET was defined as a cardiac mass with evidence of vascularity on DE-CMR, as defined by heterogeneous or diffuse contrast enhancement. CMET-positive ($CMET^+$) patients were compared with a control group of CMET-negative ($CMET^-$) patients with stage IV cancer undergoing CMR; cases and controls were matched (1:1) for primary cancer type. CMR was performed for clinical indications in both $CMET^+$ and control patients.

Comprehensive clinical data were collected in a standardized manner including cardiovascular risk factors and anticancer therapies administered within 6 months of CMR. CMR was performed between 2012 and 2015 at Memorial Sloan Kettering Cancer Center. This study was conducted with approval of the Memorial Sloan Kettering Cancer Center Institutional Review Board; the requirement for informed consent was waived.

CMR Protocol

CMR was performed on commercial (1.5 T [87%], 3.0 T [13%]) scanners (GE). Examinations consisted of 2 components—(1) cine-CMR for cardiac structure/function and (2) DE-CMR for tissue characterization. Cine- and DE-CMR images were obtained in matching short- and long-axis planes. Contiguous short-axis images were acquired from the level of the mitral annulus through the left ventricular (LV) apex. Long-axis images were acquired in 2-, 3-, and 4-chamber orientations.

Cine-CMR utilized a steady-state free precession (SSFP) pulse sequence. DE-CMR was performed post gadolinium infusion (0.2 mmol/kg) with a gradient echo inversion recovery pulse sequence; conventional (inversion time [TI] ≈300 ms) and "long TI" (TI 600 ms) were used to discern CMET vascularity. Technologists were instructed to obtain long TI DE-CMR in all patients who tolerated additional imaging beyond standard DE-CMR.

Image Analysis

CMET

CMET was scored as present or absent on a per-chamber basis (right atrium [RA], right ventricle [RV], left atrium [LA], left ventricle [LV]), as well as in the pericardium: CMET tissue characteristics and anatomic properties were assessed on CMR. Regarding tissue characterization, vascular enhancement on DE-CMR was visually scored as heterogeneous or diffuse. Heterogeneous lesions were defined based on presence of discrete regions of hyperenhancement and hypoenhancement within a single mass; diffuse lesions were defined if enhancement was present throughout the entire mass. Figure 1 provides representative CMET examples, including lesions with heterogeneous and diffuse enhancement. Signal-to-noise (SNR) and contrast-to-noise (CNR) ratios were also measured to quantitatively assess contrast-enhancement patterns. CNR and SNR were measured on "long TI" DE-CMR. For CNR, regions of maximum and minimum contrast enhancement (signal intensity) were measured by using a fixed region of interest (50 mm^2). For SNR, a single region of interest was placed over the entire mass. Regarding anatomy, cine-CMR was used to measure CMET area, perimeter, and orthogonal linear dimensions. For patients with multiple cardiac lesions, the largest mass was chosen for image analysis.

Cardiac chamber geometry

Cine-CMR was used to assess cardiac structure and function. LV and RV volumes and ejection fraction were quantified based on planimetry of end-diastolic and end-systolic short-axis slices. LV mass was quantified at end-diastole, inclusive of papillary muscles and trabeculae. LA and RA areas were measured during atrial end-diastole in 4-chamber orientation.

Examinations were also scored for pericardial and pleural effusion to assess ancillary markers of CMETs.

Mode of Spread and Prognostic Assessment

Electronic medical records and noncardiac imaging results were reviewed to evaluate overall tumor burden. Extracardiac imaging (within 6 months of CMR) was used to determine organ system involvement. Extent of disease was evaluated in

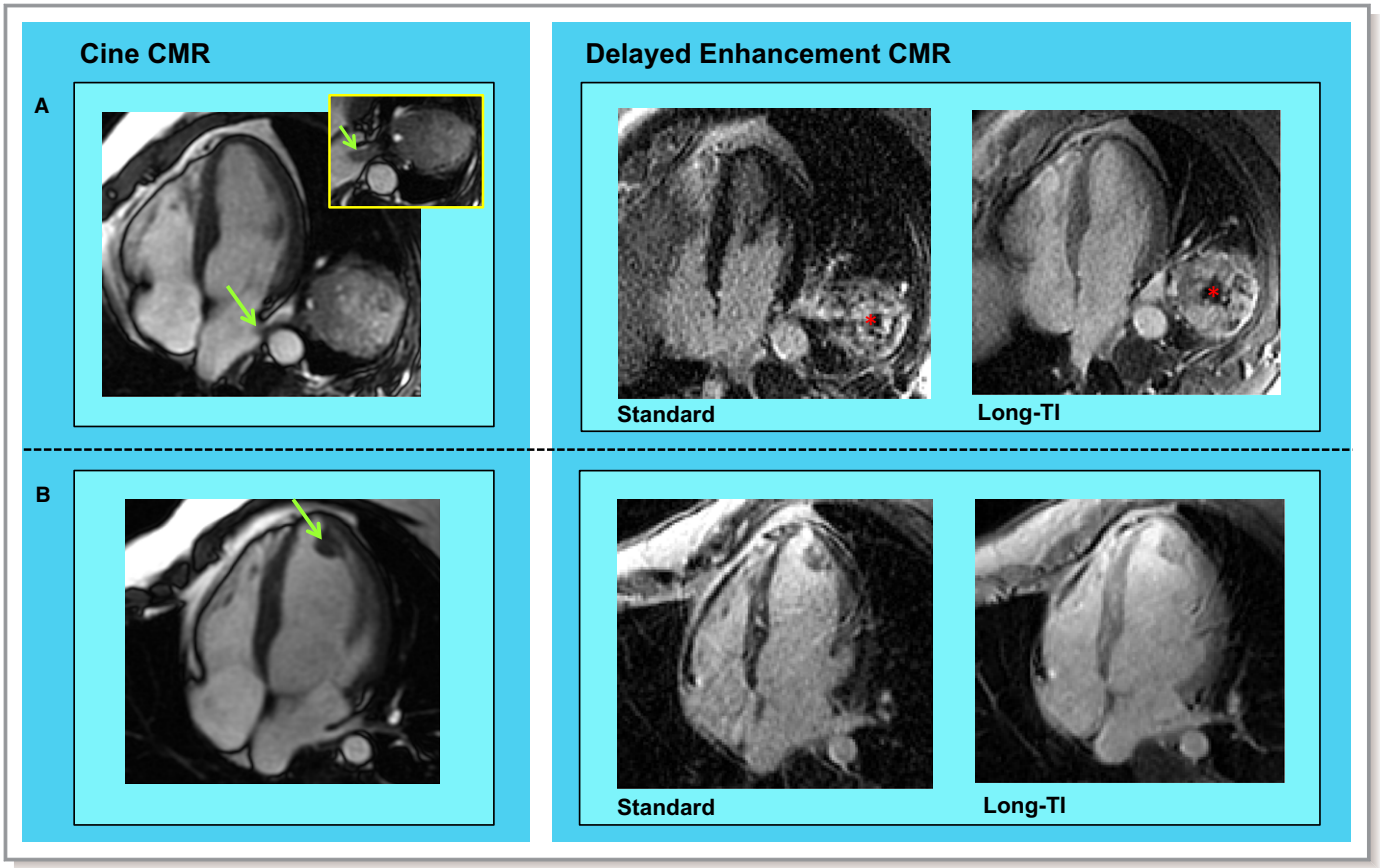

Figure 1. Cardiac metastasis (CMET) morphology and tissue properties. Representative examples of CMETs as assessed by cardiac magnetic resonance (CMR) imaging. A, Irregularly contoured left atrial mass (green arrow) in a patient with a testicular germ cell tumor. Cine-CMR (left) demonstrates direct extension via the left lower pulmonary vein. Delayed enhancement (DE-)CMR tissue characterization (right) demonstrates heterogeneous enhancement, including peripheral contrast uptake and central hypoenhancement (asterisk). B, Ovoid left ventricular apical mass (green arrow) in a patient with sarcoma. Note that whereas location and morphology on cine-CMR (left) suggest thrombus, DE-CMR tissue characterization (right) demonstrates diffuse contrast uptake—consistent with vascular supply secondary to neoplastic etiology.

accordance with established methods based on number of major organ systems involved (central nervous system, head and neck, lung, pleura, liver, gastrointestinal, genitourinary, bones or soft tissue, thoracic and abdominal lymph nodes); a cumulative scoring system was used with each organ system assigned 1 point.[12,13] Mode of spread was dichotomized as (1) hematogenous/lymphatic or (2) direct extension. Direct extension was considered present when there was tumor invasion from an adjacent site (eg, mediastinum, lung, inferior vena cava) into the heart. All other patients were considered to have CMETs as the result of hematogenous or lymphatic spread.

Electronic medical records were reviewed to assess all-cause mortality status. Time to event (death) was calculated in relation to CMR.

Statistical Methods

Comparisons between groups with or without CMETs were made by using the Student *t* test (expressed as mean±SD) for continuous variables; paired testing was performed for case–control comparisons. Categorical variables were compared by using the χ^2 or McNemar's test (for paired comparisons). Kaplan–Meier survival curves were used to compare mortality between patients with and without CMETs; follow-up duration was determined based on median (IQR) interval in relation to CMR. Statistical calculations were performed with the use of SPSS 22.0 (SPSS Inc). Two-sided $P<0.05$ was considered indicative of statistical significance.

Results

Population Characteristics

The population consisted of 60 patients with stage IV cancer (32 $CMET^+$ patients, 28 matched controls); for 4 $CMET^+$ patients (cerebellar hemipericytoma, adrenal, renal cell carcinoma [n=2]), matching was not possible because of the lack of equivalent primary cancer diagnosis among controls. Table 1 details clinical and imaging characteristics of the

Table 1. Population Characteristics

	Overall	CMET$^+$	CMET$^-$	*P* Value*
Clinical				
Age, y	58±15	60±14	57±16	0.14
Male sex	60% (36)	56% (18)	64% (18)	0.77
Disease duration, y	3.6±3.6	3.8±3.8	3.4±3.3	0.79
Cancer diagnosis				
Sarcoma	23% (14)	22% (7)	25% (7)	—
Skin cancer/melanoma	17% (10)	16% (5)	18% (5)	—
Gastrointestinal	17% (10)	16% (5)	18% (5)	—
Lung	7% (4)	6% (2)	7% (2)	—
Head and neck	7% (4)	6% (2)	7% (2)	—
Disease extent (No. of organs involved)	3.6±2.1	4.4±2.0	2.7±1.9	0.03†
Excluding cardiac involvement	3.1±2.0	3.4±2.0	2.7±1.9	0.17
Anticancer regimen				
Chemotherapy				
Alkylating agent	27% (16)	34% (11)	18% (5)	0.13
Platinum	33% (20)	41% (13)	25% (7)	0.11
Antimetabolite	25% (15)	31% (10)	18% (5)	0.23
Anthracycline	18% (11)	22% (7)	14% (4)	0.38
Topoisomerase inhibitor	18% (11)	16% (5)	21% (6)	1.00
Biologic agents	40% (24)	34% (11)	46% (13)	0.34
Radiation therapy				
Mediastinal radiation	8% (5)	9% (3)	7% (2)	1.00
Nonmediastinal radiation	25% (15)	28% (9)	21% (6)	1.00
Comorbidities				
Coronary artery disease	8% (5)	3% (1)	14% (4)	0.38
Hypertension	37% (22)	31% (10)	43% (12)	0.58
Diabetes mellitus	10% (6)	6% (2)	14% (4)	0.69
Hypercholesterolemia	20% (12)	9% (3)	32% (9)	0.07
Tobacco use	33% (20)	31% (10)	36% (10)	1.00
Cardiac morphology and function				
Left ventricle				
Ejection fraction, %	62±10	64±9	60±11	0.40
End-diastolic volume, mL	117±39	110±38	125±39	0.07
End-systolic volume, mL	45±20	41±19	50±21	0.07
Myocardial mass, g	122±66	129±84	114±38	0.72
Right ventricle				
Ejection fraction, %	52±11	51±12	53±9	0.34
End-diastolic volume, mL	137±52	130±46	146±59	0.14
End-systolic volume, mL	68±31	65±31	71±33	0.29
Atria				
Left atrial area, cm^2	20±6	19±7	21±6	0.11
Right atrial area, cm^2	21±7	20±6	22±8	0.30

*Matching not possible in 4 patients (cerebellar hemipericytoma, adrenal, renal cell carcinoma [n=2]) because of nonequivalent primary cancer diagnosis among control patients with stage IV cancer (cardiac metastasis negative [CMET]$^-$) undergoing cardiac magnetic resonance; *P*-values reflect comparisons between matched cases and controls (CMET$^+$ n=28; controls n=28).
†$P<0.05$.

population, including comparisons between patients with and without CMETs. As shown, groups were similar with respect to age, cardiovascular risk factors, and cancer treatment regimen (all *P*=NS).

Regarding extent of disease, number of noncardiac organs with metastatic cancer involvement was similar between patients with and without CMETs (3.4±2.0 versus 2.7±1.9, *P*=0.17). Of note, 94% (30/32) of patients with CMETs had metastases involving ≥1 other organ system beyond the primary tumor site and the heart (66% secondary lung metastases, 41% bones or soft tissue, 34% liver).

Anatomic and Tissue Properties

Table 2 details the anatomic distribution and mode of spread of CMETs. As shown, CMET location varied (RV 44%, n=14; RA 19%, n=6; LV 28%, n=9; LA 9%, n=3; pericardial 25%, n=8). Nearly one-fourth (22% [7/32]) of patients with CMETs had multiple cardiac chambers involved. Among patients with hematogenous or lymphatic modes of spread, right-sided chamber involvement was common (67% [14/21] RA or RV). Among patients with direct spread, the majority involved the pericardium (64% [7/11]) and cardiac chamber involvement without pericardial metastases was less common (36% [4/11]; *P*<0.001). Results also demonstrated that CMETs often occurred in the absence of ancillary findings typically associated with advanced thoracic malignancy: one-fourth (28% [n=9]) of $CMET^+$ patients had pericardial effusion; half (50% [n=16]) had pleural effusion.

Among patients with CMETs, 34% (11/32) had lesions located adjacent to ≥1 cardiac valve (tricuspid n=7, pulmonic n=4, mitral n=2). Only 2 patients had valve obstruction secondary to CMETs (both pulmonic with associated RV outflow tract obstruction).

Regarding tissue properties, CMET demonstrated heterogeneous enhancement on DE-CMR in 59% of cases (41% diffuse enhancement). Table 3 stratifies quantitative tissue properties and anatomic features in relation to visually assigned CMET enhancement patterns (heterogeneous, diffuse). As shown, heterogeneous enhancement corresponded with increased CNR (*P*<0.001), consistent with variability in contrast uptake. Heterogeneous lesions were also larger, whether measured by area, perimeter, or diameter (all *P*<0.05). Border irregularity (measured as ratio of perimeter/minimal diameter) was also greater among lesions with heterogeneous enhancement (*P*=0.006), suggestive of increased tumor growth rate.

Clinical Prognosis

Figure 2 provides Kaplan–Meier curves for groups of patients with CMETs and controls (eg, patients with stage IV cancer matched for primary diagnosis but no cardiac involvement on CMR). Median duration of post-CMR follow-up was 12.6 months (IQR 8.3–27.1) among survivors; median time to death was 5.8 months (IQR 2.2–16.7) among patients who died after CMR. Kaplan–Meier estimated survival at 6 months post-CMR was numerically lower among patients with CMET (56% [95% CI 39–74%]) compared with cancer-matched controls (68% [95% CI 50–86%]), although differences between groups were nonsignificant (*P*=0.42).

Discussion

This study provides new data concerning CMETs in patients with systemic cancer. Key findings are as follows: First, among a heterogeneous patient cohort with different cancer etiologies, CMET location varied (RV 44%, RA 19%, LV 28%, LA 9%, pericardial 25%); in nearly one-fourth (22%) of cases, CMETs involved multiple cardiac chambers. CMET location differed based on pattern of tumor metastasis to the heart; right-sided chamber involvement was common in hematologic/lymphatic spread, whereas pericardial location was common with direct spread. Second, CMETs typically occurred despite similar extracardiac metastatic disease burden compared to stage IV cancer–matched controls (organs involved 3.4±2.0 versus 2.7±1.9, *P*=0.17); 94% of CMET-affected patients had cancer involving ≥1 other organ system beyond the primary tumor site and the heart. Third, whereas CMET most often demonstrated heterogeneous enhancement on DE-CMR tissue characterization, diffuse enhancement was present in more than one-third (41%) of cases: lesions with heterogeneous enhancement demonstrated increased size and border irregularity (*P*<0.05), suggesting greater magnitude of tumor growth. Fourth, survival 6 months post CMR was numerically lower among patients with CMETs (56% [95% CI 39–74%]) compared with matched controls (68% [95% CI 50–86%]), although differences between groups were nonsignificant (*P*=0.42).

Our results—obtained in vivo by using DE-CMR tissue characterization—extend prior research that has used autopsy data or imaging to evaluate pattern and tissue manifestations of CMETs. Consistent with our finding of varying CMET location, Bussani et al reported that among 662 patients with autopsy-evidenced CMETs, lesions were dispersed throughout the pericardium (69%), epicardium (34%), myocardium (32%), and endocardium (5%)—although location of cardiac chamber involvement was not defined.[14] Among 110 patents with autopsy-proved CMET, Klatt and Heitz reported that lung carcinoma, breast carcinoma, melanoma, and lymphoma were the most common tumor etiologies, similar to data from other autopsy data reports.[1,15] Our study includes CMETs among patients with cancers conventionally

Table 2. Anatomic Distribution of Cardiac Metastases

Diagnosis	Mode of Spread (1=Heme/Lymph, 2=Direct)	Cardiac Involvement Pattern					Effusion	
		LV	RV	LA	RA	Pericardium	Pericardial	Pleural
Musculoskeletal								
Liposarcoma (paraspinal)	2	—	—	—	—	X	—	—
Solitary fibrous tumor (neck)	2	—	X	—	—	X	X	—
Osteoarcoma (thigh)	1	—	—	X	—	—	—	X
Myxofibrosarcoma (axilla)	1	—	X	—	—	—	X	X
Synovial sarcoma (unknown primary)	1	X	—	X	—	—	—	—
Myxofibrosarcoma (thigh)	1	X	—	—	—	—	—	—
Dermatologic								
Melanoma	1	—	X	—	—	—	—	—
Melanoma	1	—	—	—	X	—	—	—
Melanoma	1	—	—	—	X	—	—	—
Melanoma	1	—	—	—	—	X	X	—
Merkel cell carcinoma	1	—	—	—	X	—	—	X
Gastrointestinal								
Gastrointestinal stromal tumor	2	—	—	—	—	X	X	X
Pancreatic adenocarcinoma	1	—	X	—	—	—	—	X
Pancreatic adenocarcinoma	1	—	X	—	—	—	—	X
Pancreatic adenocarcinoma	1	—	X	—	X	—	—	X
Hepatocellular carcinoma	2	—	—	—	X	—	—	—
Lung								
Non–small cell lung	2	—	—	—	—	X	—	X
Non–small cell lung	1	—	X	—	—	—	—	X
Bronchial carcinoid	1	X	X	—	—	—	—	—
Leiomyosarcoma (pulmonary artery)	2	—	X	—	—	—	—	—
Other								
Renal cell carcinoma	1	X	—	—	—	—	—	—
Renal cell carcinoma	2	—	—	—	X	—	—	X
Renal cell carcinoma	1	—	X	—	—	—	—	X
Germ cell (mediastinal)	2	—	—	—	—	X	X	X
Germ cell (testicular)	2	—	—	X	—	—	—	—
Tongue squamous cell	1	X	X	—	—	—	X	X
Parotid adenosquamous	1	—	X	—	—	—	X	—
Thymic carcinoid	2	X	X	—	—	X	X	X
Breast carcinoma	1	X	—	—	—	—	X	X
Diffuse large B-cell lymphoma	2	—	—	—	—	X	—	X
Adrenal carcinoma	1	X	—	—	—	—	—	—
Cerebellar hemangiopericytoma	1	X	X	—	—	—	—	—

LA indicates left atrium; LV, left ventricle; RA, right atrium; RV, right ventricle.

associated with cardiac involvement (eg, melanoma, lung, breast) as well as atypical cancer etiologies (eg, central nervous system, adrenal, hepatocellular). Among a cohort of pediatric osteosarcoma patients, Yedururi et al used computed tomography and magnetic resonance imaging to demonstrate that cardiovascular metastases typically involved

Table 3. Postcontrast Tissue Characteristics and Anatomic Features of Cardiac Metastases

	Overall	Diffuse Enhancement	Heterogeneous Enhancement	*P* Value
Anatomic features				
Maximal diameter, cm	5.0±3.6	2.4±1.1	6.1±3.2	0.001†
Minimal diameter, cm	2.9±2.1	1.6±0.9	3.3±2.0	0.013†
Area, cm^2	16.2±22.8	3.5±2.9	19.3±22.1	0.021†
Perimeter, cm	15.1±12.5	6.7±3.1	17.5±9.8	0.001†
Perimeter/minimal diameter	5.0±1.4	4.3±1.0	5.6±1.4	0.006†
Tissue properties*				
Contrast-to-noise ratio	9.8±9.1	2.6±2.4	14.9±8.6	<0.001†
Signal-to-noise ratio	30.8±25.5	36.1±30.8	27.0±21.2	0.39

*Quantification of contrast-enhanced tissue properties via dedicated "long TI" delayed enhancement cardiac magnetic resonance possible in 91% (29/32) patients (long TI not obtained in 3 patients because of inability to tolerate full cardiac magnetic resonance protocol).
†$P<0.05$.

pulmonary arteries or pulmonary veins, although a minority (6 of 20) involved cardiac chambers.[16] Taken together, these findings highlight the need for comprehensive surveillance of cardiac involvement regardless of cancer etiology.

To the best of our knowledge, this is the first CMR study to primarily examine cardiac manifestations of systemic cancer. Prior studies have used CMR to study cardiac neoplasms in mixed cohorts, among whom DE-CMR has been used as the reference for tumor vascularity. In 116 patients with cardiac masses, Pazos-Lopez et al. demonstrated that the absence of contrast uptake on DE-CMR was useful for differentiating thrombus from neoplasm.[11] However, in this cohort, only 22% of patients had malignant tumors. Similarly, among a cohort of 78 pediatric patients, Beroukhim et al used CMR to demonstrate that malignant tumors demonstrated tumor vascularity on the basis of postcontrast properties—however, fewer than one-fifth had cardiac malignancies in the context of systemic cancer.[10] Other studies have similarly used DE-CMR to assess tumor vascularity but did so exclusively among patients with primary cardiac tumors.[17] These prior data demonstrate that DE-CMR tissue characterization is useful for identification of neoplasms. However, results have been limited concerning manifestations of secondary cardiac tumors, which are much more common than primary cardiac malignancies.[18]

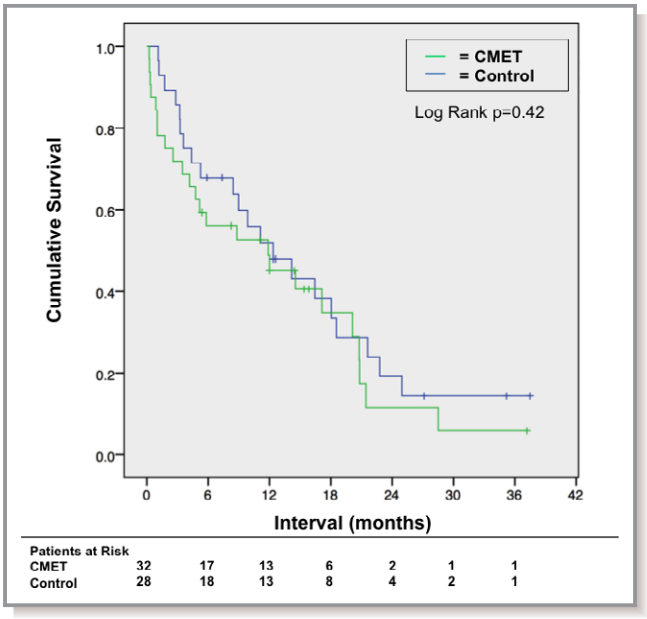

Figure 2. Mortality status. Kaplan–Meier curves for patient groups partitioned based on cardiac metastasis (CMET) status (green=$CMET^+$, blue=controls [$CMET^-$ stage IV cancer patients matched for primary cancer etiology]). Note similar mortality status between groups (P=0.42).

An important aspect of our study concerns our finding that contrast-enhanced tissue properties of CMET can vary, with some tumors demonstrating diffuse enhancement and others showing heterogeneous enhancement. Visual scoring corresponded with quantitative results; higher CNR (calculated based on differential signal intensity between maximally and minimally enhancing regions) is consistent with marked differences in contrast uptake within a given lesion. Regarding mechanism, we speculate that focal hypoenhancement corresponds to areas of decreased vascularity and/or tumor necrosis. Consistent with this notion, animal studies have demonstrated that regions of tumor necrosis (on pathology) correlated with deceased perfusion on CMR and reduced metabolic activity on positron emission tomography.[19] Studies have also indicated that tumor necrosis corresponds to chronic ischemic injury from tissue hypoxia, which would be

expected to manifest as decreased contrast uptake on DE-CMR.[20,21] Our finding of increased border irregularity and lesion size among patients with heterogeneous enhancement supports the notion that necrosis may be due to tumor aggressiveness, resulting in cell death as a result of vascular supply–demand mismatch with resultant hypoenhancement on DE-CMR.

Several limitations should be noted. First, it is important to recognize that this study cohort was accrued from patients referred for clinical CMR, and thus findings cannot be used to determine the overall prevalence of CMETs. On the other hand, CMET-affected patients were matched to unaffected controls (with matched diagnoses), thereby providing a valuable cohort with which to compare functional, structural, and prognostic manifestations of CMETs. Second, whereas results demonstrate nonsignificant differences in prognosis between patients with CMET and matched controls, our relatively small sample size may have blurred distinctions between groups. Larger population-based studies examining all-cause mortality and cardiac-specific events (eg, heart failure, arrhythmia) are needed to examine this issue. It is also important to note that our study assessed CMETs via a conventional breath-held segmented inversion recovery pulse sequence, so as to test a widely available CMR tissue characterization approach. Alternative free breathing pulse sequences such as single shot and navigator gated 3-dimensional imaging, as well as phase-sensitive reconstruction techniques, may enable simplified CMR protocols that are robust and well tolerated—features of particular relevance given the clinical frailty of patients with advanced cancer.[22–24] Further, while this is the first study to report imaging features of CMETs among a broad array of cancer etiologies and to assess the prognosis of patients with CMET compared with diagnosis-matched cancer patients with a similar extent of systemic disease (but no cardiac involvement), it should be noted that all patients were derived from a single tertiary care cancer center. Future research encompassing a larger patient cohort derived from multiple institutions is warranted to further validate current findings.

In conclusion, results from this study demonstrate that CMETs can vary with respect to cancer type, cardiac location, and tissue properties. Despite advances in cancer care, prognosis of CMET-affected patients remains poor—further studies are warranted to assess optimal treatment strategies based on etiology and tissue properties of CMETs.

Sources of Funding

This research was funded in part through the National Institutes of Health/National Cancer Institute Cancer Center Support Grant P30 CA008748.

Disclosures

None.

References

1. Klatt EC, Heitz DR. Cardiac metastases. *Cancer*. 1990;65:1456–1459.
2. Lam KY, Dickens P, Chan AC. Tumors of the heart. A 20-year experience with a review of 12,485 consecutive autopsies. *Arch Pathol Lab Med*. 1993;117:1027–1031.
3. Yusuf SW, Bathina JD, Qureshi S, Kaynak HE, Banchs J, Trent JC, Ravi V, Daher IN, Swafford J. Cardiac tumors in a tertiary care cancer hospital: clinical features, echocardiographic findings, treatment and outcomes. *Heart Int*. 2012;7:e4 doi: 10.4081/hi.2012.e4. Epub February 13, 2012.
4. Weinsaft JW, Kim RJ, Ross M, Krauser D, Manoushagian S, LaBounty TM, Cham MD, Min JK, Healy K, Wang Y, Parker M, Roman MJ, Devereux RB. Contrast-enhanced anatomic imaging as compared with contrast-enhanced tissue characterization for detection of left ventricular thrombus. *JACC Cardiovasc Imaging*. 2009;2:969–979.
5. Weinsaft JW, Kim HW, Crowley AL, Klem I, Shenoy C, Van Assche L, Brosnan R, Shah DJ, Velazquez EJ, Parker M, Judd RM, Kim RJ. LV thrombus detection by routine echocardiography: insights into performance characteristics using delayed enhancement CMR. *JACC Cardiovasc Imaging*. 2011;4:702–712.
6. Grothues F, Smith GC, Moon JC, Bellenger NG, Collins P, Klein HU, Pennell DJ. Comparison of interstudy reproducibility of cardiovascular magnetic resonance with two-dimensional echocardiography in normal subjects and in patients with heart failure or left ventricular hypertrophy. *Am J Cardiol*. 2002;90:29–34.
7. Weinsaft JW, Kim HW, Shah DJ, Klem I, Crowley AL, Brosnan R, James OG, Patel MR, Heitner J, Parker M, Velazquez EJ, Steenbergen C, Judd RM, Kim RJ. Detection of left ventricular thrombus by delayed-enhancement cardiovascular magnetic resonance prevalence and markers in patients with systolic dysfunction. *J Am Coll Cardiol*. 2008;52:148–157.
8. Srichai MB, Junor C, Rodriguez LL, Stillman AE, Grimm RA, Lieber ML, Weaver JA, Smedira NG, White RD. Clinical, imaging, and pathological characteristics of left ventricular thrombus: a comparison of contrast-enhanced magnetic resonance imaging, transthoracic echocardiography, and transesophageal echocardiography with surgical or pathological validation. *Am Heart J*. 2006;152:75–84.
9. Kirkpatrick JN, Wong T, Bednarz JE, Spencer KT, Sugeng L, Ward RP, DeCara JM, Weinert L, Krausz T, Lang RM. Differential diagnosis of cardiac masses using contrast echocardiographic perfusion imaging. *J Am Coll Cardiol*. 2004;43:1412–1419.
10. Beroukhim RS, Prakash A, Buechel ER, Cava JR, Dorfman AL, Festa P, Hlavacek AM, Johnson TR, Keller MS, Krishnamurthy R, Misra N, Moniotte S, Parks WJ, Powell AJ, Soriano BD, Srichai MB, Yoo SJ, Zhou J, Geva T. Characterization of cardiac tumors in children by cardiovascular magnetic resonance imaging: a multicenter experience. *J Am Coll Cardiol*. 2011;58:1044–1054.
11. Pazos-Lopez P, Pozo E, Siqueira ME, Garcia-Lunar I, Cham M, Jacobi A, Macaluso F, Fuster V, Narula J, Sanz J. Value of CMR for the differential diagnosis of cardiac masses. *JACC Cardiovasc Imaging*. 2014;7:896–905.
12. Gerdan L, Segedin B, Veninga T, Schild SE, Rades D. Number of involved extracranial organs predicts survival in patients with brain metastasis from small cell lung cancer. *Anticancer Res*. 2013;33:3887–3889.
13. Hendriks LE, Derks JL, Postmus PE, Damhuis RA, Houben RM, Troost EG, Hochstenbag MM, Smit EF, Dingemans AM. Single organ metastatic disease and local disease status, prognostic factors for overall survival in stage IV non-small cell lung cancer: results from a population-based study. *Eur J Cancer*. 2015;51:2534–2544.
14. Bussani R, De-Giorgio F, Abbate A, Silvestri F. Cardiac metastases. *J Clin Pathol*. 2007;60:27–34.
15. Butany J, Leong SW, Carmichael K, Komeda M. A 30-year analysis of cardiac neoplasms at autopsy. *Can J Cardiol*. 2005;21:675–680.
16. Yedururi S, Morani AC, Gladish GW, Vallabhaneni S, Anderson PM, Hughes D, Wang WL, Daw NC. Cardiovascular involvement by osteosarcoma: an analysis of 20 patients. *Pediatr Radiol*. 2016;46:21–33.
17. Kaminaga T, Takeshita T, Kimura I. Role of magnetic resonance imaging for evaluation of tumors in the cardiac region. *Eur Radiol*. 2003;13(suppl 6):L1–L10.
18. Butany J, Nair V, Naseemuddin A, Nair GM, Catton C, Yau T. Cardiac tumours: diagnosis and management. *Lancet Oncol*. 2005;6:219–228.
19. Cho H, Ackerstaff E, Carlin S, Lupu ME, Wang Y, Rizwan A, O'Donoghue J, Ling CC, Humm JL, Zanzonico PB, Koutcher JA. Noninvasive multimodality imaging of the tumor microenvironment: registered dynamic magnetic resonance

imaging and positron emission tomography studies of a preclinical tumor model of tumor hypoxia. *Neoplasia*. 2009;11:247–259, 242p following 259

20. Swinson DE, Jones JL, Richardson D, Cox G, Edwards JG, O'Byrne KJ. Tumour necrosis is an independent prognostic marker in non-small cell lung cancer: correlation with biological variables. *Lung Cancer*. 2002;37:235–240.
21. Pollheimer MJ, Kornprat P, Lindtner RA, Harbaum L, Schlemmer A, Rehak P, Langner C. Tumor necrosis is a new promising prognostic factor in colorectal cancer. *Hum Pathol*. 2010;41:1749–1757.
22. Piehler KM, Wong TC, Puntil KS, Zareba KM, Lin K, Harris DM, Deible CR, Lacomis JM, Czeyda-Pommersheim F, Cook SC, Kellman P, Schelbert EB. Free-breathing, motion-corrected late gadolinium enhancement is robust and extends risk stratification to vulnerable patients. *Circ Cardiovasc Imaging*. 2013;6:423–432.
23. Kellman P, Arai AE, McVeigh ER, Aletras AH. Phase-sensitive inversion recovery for detecting myocardial infarction using gadolinium-delayed hyper-enhancement. *Magn Reson Med*. 2002;47:372–383.
24. Nguyen TD, Spincemaille P, Weinsaft JW, Ho BY, Cham MD, Prince MR, Wang Y. A fast navigator-gated 3D sequence for delayed enhancement MRI of the myocardium: comparison with breathhold 2D imaging. *J Magn Reson Imaging*. 2008;27:802–808.